Electrochemical Fabrication of 2D CuO Nanosheets on Pt for Highly Sensitive Non-enzymatic Bio-sensing of Glucose.

Jagdish C. Bhangoji[a], Christopher J. Barile[b] and Suresh S. Shendage[*a].
[a]Dept. Of Chemistry, V. G. Vaze College of Arts, Science and Commerce (Autonomous), Mithagar Road, Mulund (E), Mumbai - 400081. (Maharashtra) India
[b]Department of Chemistry, University of Nevada, Reno, Reno, NV, USA
Email - sureshsshendage@gmail.com

Abstract

A simple and environmentally-friendly approach was developed to synthesize 2D CuO nanosheets using electrochemical deposition. The formed 2D CuO nanosheets (NSs) exhibit numerous advantageous properties such as nontoxicity, high electrical conductivity, large active surface area, and a p-type semiconducting nature with a band gap of 1.2 eV. A sensitive electrochemical sensor was constructed for the amperometric detection of glucose to take advantage of these characteristics. The fabricated sensor displayed an excellent sensitivity of 2710 $mA.mM^{-1}.cm^{-2}$ along with a wide linear range of 0.001–1.0 mM and a lower limit of detection of 0.8 μM (S/N = 3). Additionally, the modified electrode possesses high selectivity and good stability. The outstanding electrocatalytic performance of the electrode is attributed to a large active surface area, unique structural morphology, and the high conductivity of the 2D CuO nanosheets. Moreover, the sensor was successfully employed for the amperometric detection of glucose in blood samples, demonstrating its potential practical utility.

Keywords: Cyclic voltammetry, sensor, CuO, nanosheets, glucose.

1. Introduction

Glucose is one of the major sources of energy for humans and is a fundamental part of blood serum [1]. The standard level of body glucose in a healthy person ranges from 3.9-6.1 mM, while levels higher than 6.1 mM are indicative of diabetes mellitus [2]. Diabetes is caused by an increase in blood glucose concentration (hyperglycemia) that originates from a lack of insulin secretion that decreases glucose metabolism [3-4]. For the clinical diagnosis and management of diabetes, controlling glucose levels is essential [5]. For this reason, the fast, accurate, sensitive, and selective detection of blood glucose is important for the diagnosis and management of diabetes.

A wide variety of analytical techniques including fluorometry, oxidimetry, titrimetry, colorimetry, chemiluminescence, chromatography, spectrophotometry, and electrochemical sensors have been employed for the detection of glucose [6-8]. Aside from electrochemical sensors, these techniques are expensive, suffer from poor sensitivity, are unreliable, or have complex operating procedures [7]. In contrast, electrochemical techniques have been extensively used for the detection of glucose because this approach is simple, fast, comparatively inexpensive, highly sensitive, consistent, and suitable for the quantitative detection of glucose [1,8-9].

Electrochemical sensors are commonly classified as enzymatic and non-enzymatic sensors. Due to their high sensitivity and selectivity, enzymatic sensors have received much research attention. However, enzymes suffer from several drawbacks including the instability of enzymes, sensitivity associated with environmental factors, relatively high cost, the need for complex immobilization procedures and electron mediators, non-recyclability for subsequent analysis due to deposition of serum proteins and interferent species in blood serum [2,10]. To overcome these shortcomings, non-enzymatic electrochemical sensors are a promising alternative for the detection and measurement of glucose [9-11].

In the last decade, noble metals in the form of Ag nanoparticles (NPs) [12-13], Au NPs [14-16], Pt NPs [17-19], Pd NPs [20-21], and noble metal alloys [22-24] have been employed for the fabrication of glucose sensors because they have high conductivity and excellent catalytic activity. Nonetheless, these materials based on noble metals possess several disadvantages including poisoning of Au and Pt by the absorption of intermediates and chloride ions, which impedes electron transfer and ultimately reduces the sensitivity and selectivity of the sensors. These sensors also possess low working stability and are relatively expensive [2-3,4,25]. For these reasons, there is great interest in developing non-enzymatic glucose sensors based on earth-abundant and low-cost transition metal oxides.

Currently, several low-cost transition metal oxides such as Fe_2O_3 [26-27], Mn_xO_x [6, 28], MoO_2 [29], CdO [30], NiO [1-2, 31-32], ZnO [33-34], and CuO [25, 35] have been studied for use in non-enzymatic glucose sensors. Among all of these metal oxides, CuO has been widely explored as a catalytic material for different applications including semiconductors, supercapacitors, batteries, solar energy conversion, gas sensing devices, catalysis, biosensors, and transistors because it is a p-type semiconductor with a band gap of 1.2 eV, and it exhibits a low overpotential for electron exchange, excellent electrocatalytic activity, high active surface area, good chemical stability, and biocompatibility. Additionally, CuO is nontoxic, inexpensive, and abundant [25, 35-36].

The particle size and shape of materials significantly affect their electrocatalytic activity [25]. CuO nanomaterials of various shapes have been designed and studied for glucose sensing applications including nanospheres [48], nanorods [49], nanowires [39-40], nanocubes [41], nanosheets [42-43], nanofibers [44], nanoflowers [25,45], and octahedra [46-47]. In addition, the fabrication of electrodes for non-enzymatic sensors by a drop casting process through the help of costly binder polymer solutions possesses some disadvantages. First, polymer binder solutions may block the electroactive sites of the catalytic materials, and accordingly decrease the catalytic activity of the materials. Second, catalytic materials can desorb off of the electrode during the electrochemical reactions. Third, the binder solutions significantly decrease the electrical conductivity of the electrode. To overcome these issues, sensor electrodes designed by direct deposition of catalytic materials on the electrode surface with well-defined morphological shape are of great interest for the non-enzymatic detection of biomolecules [48].

In this work, we report non-enzymatic electrochemical sensors based on 2D CuO nanosheets electrochemically deposited on Pt foil for the detection of glucose. The synthesized materials were characterized by FE-SEM, HR-TEM, XRD, and cyclic voltammetry techniques. The fabricated 2D CuONSs@Pt foil sensors exhibit high sensitivity, excellent selectivity, and stability with good reproducibility due to the morphology of the 2D nanostructures and large active surface area of the CuO NSs. The effects of different synthetic parameters on the morphology and catalytic activity were also investigated. Generally, it was found that the size, morphology and electrocatalytic performance strongly depend upon the concentration of Cu^{2+} ions, deposition time, deposition potential, and solution pH.

2. Experimental

2.1 Reagents and Chemicals

Cupric nitrate trihydrate [$Cu(NO_3)_2.3H_2O$] (SD-Fine chem India), sodium hydroxide (SD-Fine chem India), H_2O_2, ethanol, ascorbic acid, dopamine, uric acid, KCl, NaCl, and all other chemicals were of analytical grade and used without additional purification. All of the solutions and reagents were prepared using ultra-pure water.

2.2 Instruments

Electrochemical experiments were conducted using a Potentiostat-galvanostat DY2300 series Potentiostat electrochemical workstation (Austin, TX, USA) with a conventional three-electrode system. The CuO@Pt foil (3×3 mm^2) was used as the working electrode, a glassy carbon electrode (GCE, 3 mm) was used as the auxiliary electrode, and a saturated calomel electrode (SCE) was used as the reference electrode, respectively. All potentials in this manuscript are reported versus SCE. Materials characterization was performed using an HR-transmission electron microscope (HR-TEM, JEOL, JEM 2100F) operated at 10 kV and a field emission gun scanning electron microscope (FEG-SEM, JSM-7600F) operated at 10 kV. The X-ray diffraction (XRD) analysis was performed with a PANalytical, Netherlands (k_αCu - 1.54184 A^o) instrument.

Galvanostatic Deposition and Fabrication of 2D CuONSs@Pt Foil Electrode

Commercially purchased Pt foil (3×3 mm^2) was thoroughly polished with a slurry of 0.05 μm alumina powder and water. The Pt was then successively sonicated in 0.1 M HCl, deionized water, and absolute ethanol for 5 min each. A precursor $Cu(NO_3)_2$ solution (10 mM) was placed in two 100 cm^3 of beakers. 0.1 M NaOH was slowly added to one beaker with constant stirring, and 0.1 M HNO_3 was slowly added to the other beaker to form $Cu(OH)_2$ and $Cu(NO_3)_2$, respectively. The precursor solutions were then vigorously stirred for an additional 15 min to avoid agglomeration and ensure uniform mixing. Cleaned Pt foil was then immersed in each of the two beakers and connected to the -ve terminal (cathode) of a DC power supply. At the same time, a stainless steel rod (2 mm) was connected to the +ve terminal (anode) of the power supply. Both the electrodes were kept at a distance of approximately 2 cm. A constant potential of 1.5 V was applied to deposit CuO on the Pt electrode. The CuO-modified electrode was then rinsed with deionized water and dried in oven at 150 ^oC. The electrode was then used for electrochemical studies. An overview of the electrodeposition process of the 2D CuO NSs and their electrochemical sensing application for glucose is displayed in **Scheme 1**.

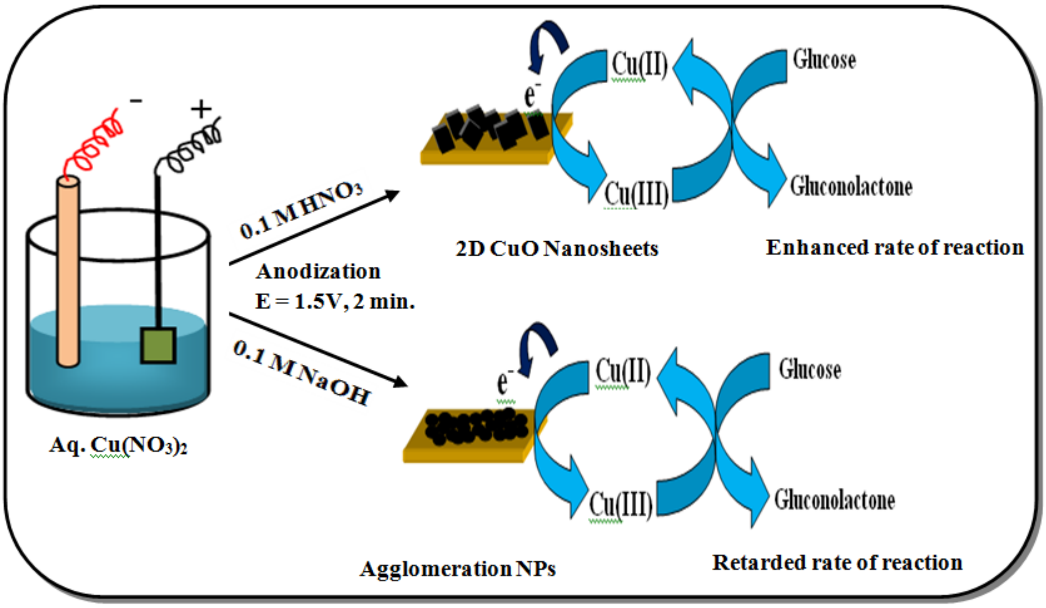

Scheme1. Synthesis of 2DCuO NSs and application for electrooxidation of glucose.

3. Results and Discussion

3.1 Structural Analysis

The simultaneous electrochemical exfoliation and deposition of CuO nanostructures on Pt foil is a straight forward approach to design modified electrodes for glucose sensing. The morphology of the synthesized nanostructure was examined by FE-SEM and FE-TEM scanning microscopic techniques. When synthesized under alkaline conditions (0.1 M NaOH), large agglomerates of CuO nanoparticles were observed **(Fig 1A)**. However, when CuO was synthesized in acid (0.1 M HNO_3), sheet structures were formed instead of agglomerates **(Fig. 1B)**. A high-resolution TEM image indicates that a large amount of 2D CuO sheets are uniformly spread over the surface of the Pt electrode and that the nanosheets are about 10-15 nm in size **(Fig. 1C)**.

X-ray diffraction (XRD) was used to further interrogate the structure of the synthesized nanomaterials (**Fig. 1D)**. Sharp and intense diffraction peaks observed at 2θ = 32.5°, 35.5°, 38.7°, 48.8°, 53.5°, 58.2°, 61.5°, 66.2°, and 68.1° correspond to (110), (-111), (111), (-202), (020), (202), (-113), (-311), and (220) crystal planes of monoclinic CuO (JCPDS 41-0254), respectively. In addition, the diffraction peaks at 2θ = 29.7°, 42.4°, and 73.9° are due to the cubic phase of Cu_2O. From the above XRD results, it can be concluded that 2D CuO nanosheets material is successfully synthesized along with small amount of Cu_2O. The nature of the material is crystalline [49-50]. The crystallite size is determined by using Scherer equation as given below

$$D = K\lambda/\beta cos\theta \qquad \text{.......................... (eq. 1)}$$

where, D, K, λ, β, and θ are the crystal size (nm), Scherer constant, X-ray wavelength (nm), half width full maxima (radians), and angle of diffraction (degree), respectively. From this equation, the crystal size was calculated to be 14.73 nm, which matches well with the 10-15 nm particles observed in the HR-TEM image.

3.2 Electrochemically Active Surface Area (EASA)

The electrochemically active surface area (EASA) of Pt electrode modified with CuO NSs was determined by measuring cyclic voltammograms (CVs) in 20 mM $K_3[Fe(CN)_6]$ and 0.1 M KCl at a scan rate of 50 mVs^{-1}. CVs for bare Pt and Pt modified with CuO nanosheets are shown in **Fig. 2**. The active surface area was calculated using the Randles–Sevcik equation given below [51].

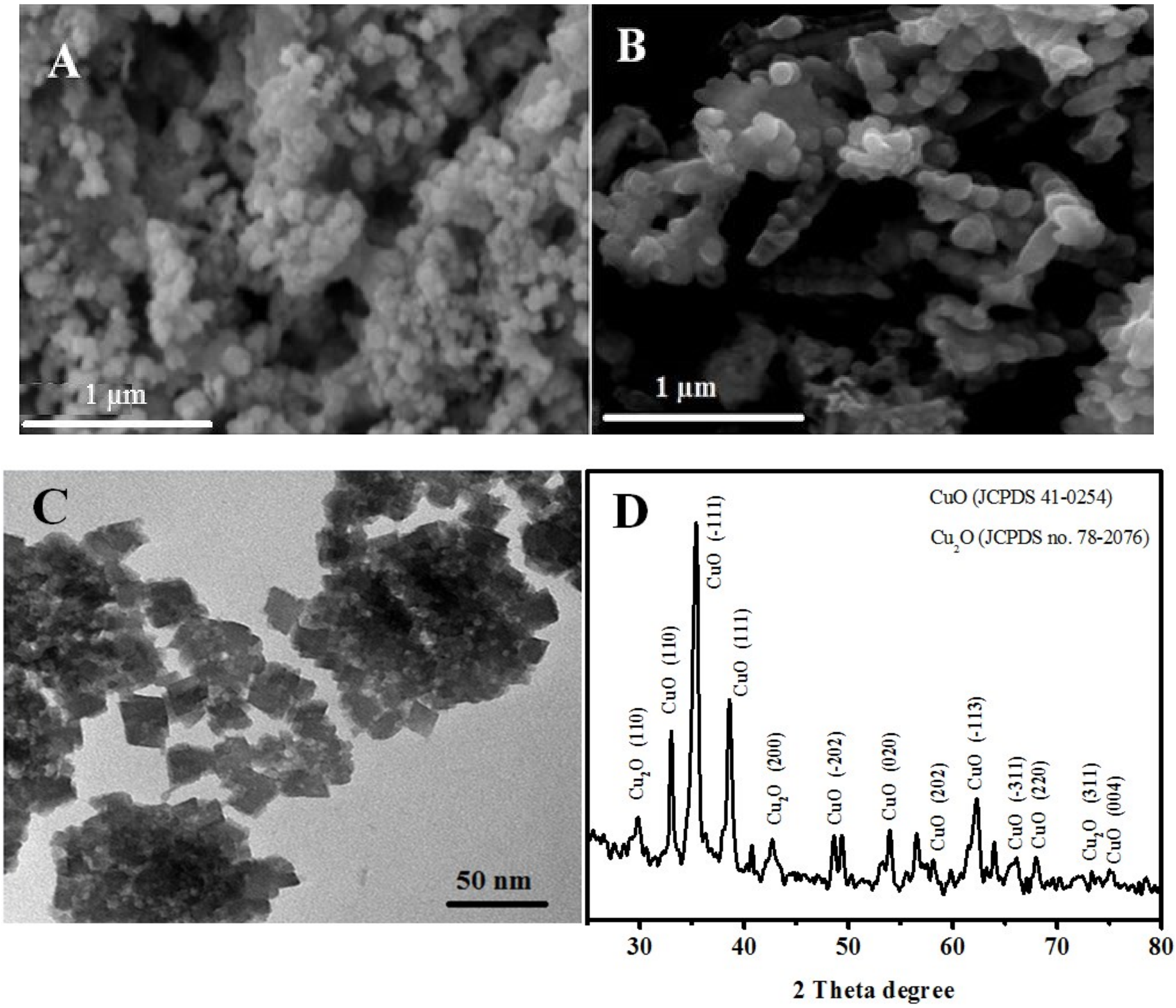

Figure 1. FE-SEM images of CuO NPs synthesized in alkaline medium **(A)**, 2D nanosheets synthesized in acidic medium **(B)**, HR-TEM image of 2D CuO NSs **(C)**, and XRD pattern of CuO NSs materials **(D)**.

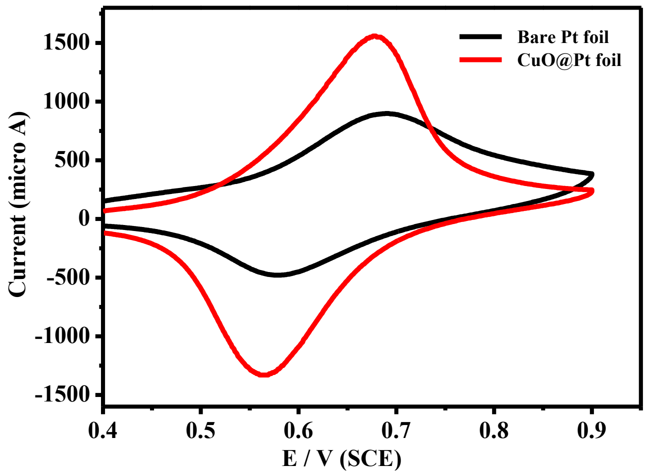

Figure 2. Cyclic voltammograms of (black line) bare Pt foil and (red line) 2D CuONSs@Pt foil electrode in 20 mM $K_3[Fe(CN)_6]$ and 0.1 M KCl solution at a scan rate of 50 mVs^{-1}.

$I_p = 2.69\times10^5\times n^{3/2}\times A\times D^{1/2}\times v^{1/2}\times C$ ($n=1$, $D=0.76\times10^{-5} cm^2s^{-1}$, $v=0.05\ Vs^{-1}$)............(eq. 2)

where, I_p, n, A, D, v, and C are the peak current (μA), number of electrons transferred in the redox reaction, electrode area (cm^2), diffusion coefficient (cm^2s^{-1}), scan rate (mVs^{-1}), and concentration of the analyte (mM), respectively. The active surface areas of the bare and CuO-modified-electrodes were found to be 0.2755 cm^2 and 0.4768 cm^2, respectively. In contrast, the geometric surface area of the bare Pt foil electrode is only 0.09 cm^2. These results demonstrate that the active surface area of the Pt foil electrode after electrochemical deposition of CuO nanosheets is greatly increased, which is advantageous to accelerate the glucose oxidation reaction.

3.3 Electrocatalytic Activity of 2D CuONSs@Pt Foil towards Glucose

Fig. 3 illustrates cyclic voltammograms of bare Pt foil and 2D CuONSs@Pt foil in the presence **(Fig. 3A)** and absence **(Fig. 3B)** of 2 mM glucose in 0.1 M NaOH as a supporting electrolyte solution at a potential range of -0.2 V to 0.8 V at a scan rate of 50 mVs^{-1}. Notably, bare Pt foil exhibits no redox peaks in the absence of glucose (**Fig. 3B, black line**). However, a well-defined peak is seen at 0.48 V for the 2D CuONSs@Pt foil electrode (**Fig. 3B, red line**). This peak is attributed to the reduction of Cu(III) to Cu(II). The corresponding oxidation of Cu(II) to Cu(III) does not result in a peak because it is masked due to the simultaneous O_2 evolution reaction from water splitting [47]. Upon addition of 2 mM glucose to the electrolyte, oxidation peaks are observed at 0.42 V for the 2D CuONSs@Pt foil electrode (acidic medium) with increased oxidation current as compared to bare Pt and the Pt modified with CuNPs (alkaline medium, **Fig. 3A**).This difference in the current density of the oxidation peaks is due to the difference in morphology of the CuO nanomaterial. The agglomerated particles when the CuO is synthesized in base result in a decreased surface area of the catalytic material. In contrast, when the CuO is synthesized in acid, 2D nanosheets are formed, which increase the electrochemical active surface area and correspondingly increase the rate of the glucose oxidation reaction.

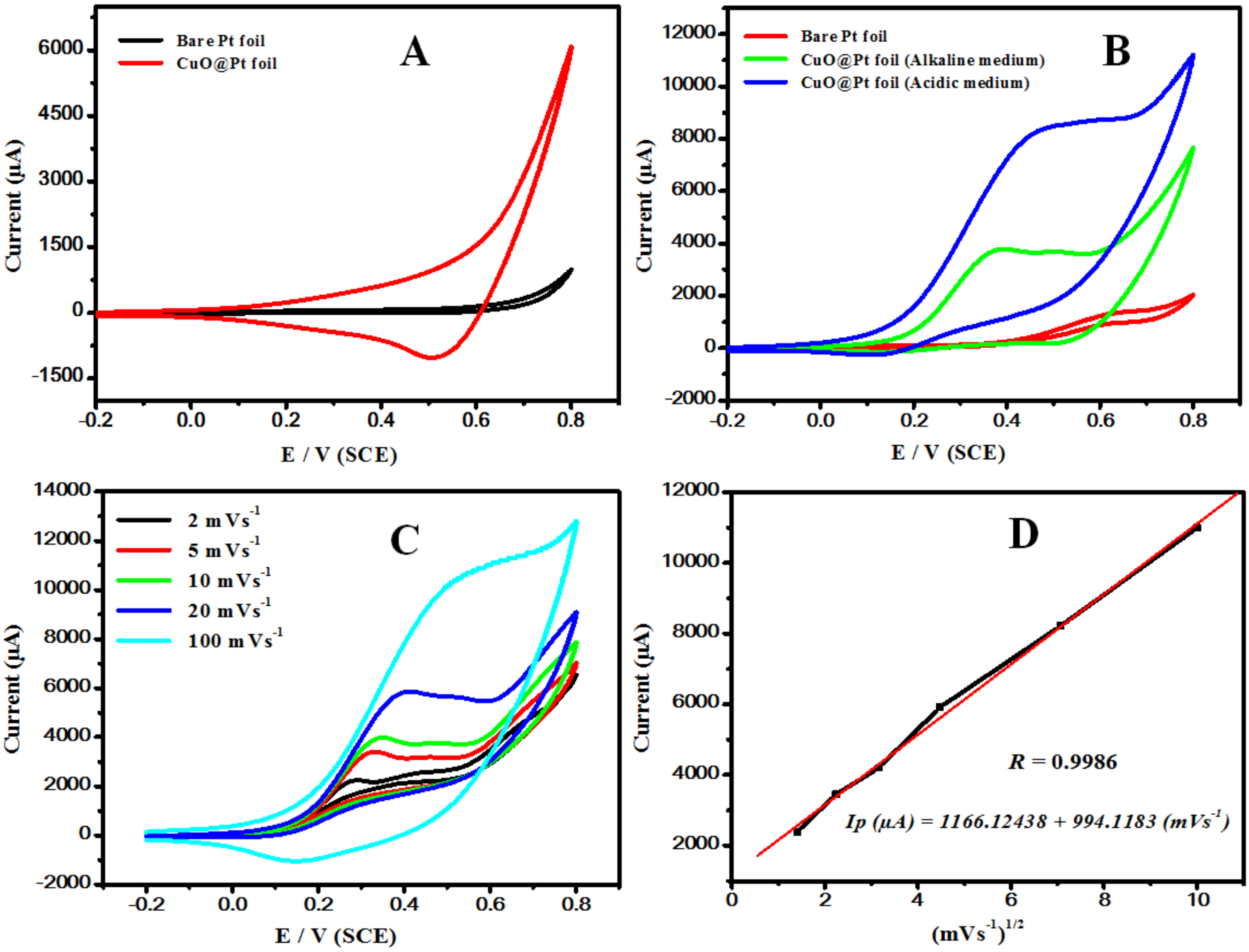

Figure 3. CVs of bare Pt foil and 2D CuO NSs modified Pt foil electrodes in the presence **(A)** and absence **(B)** of 2 mM glucose in 0.1 M NaOH electrolyte solution at a scan rate of 50 mVs^{-1}, **(C)** CVs of CuONSs@Pt foil electrode at different scan rates ranging from (2, 5, 10, 20, 50 and 100 mVs^{-1}) in 2 mM glucose + 0.1 M NaOH and **(D)** corresponding linear plot of square root of scan rate versus oxidation current.

The redox mechanism of the 2D CuO nanosheets and glucose is displayed in the following equations. In the first step, $Cu(OH)_2$ is oxidized to CuOOH. In the second step, CuOOH oxidizes glucoses, regenerating $Cu(OH)_2$ in the process (36).

$$Cu(OH)_2 + OH^- \longrightarrow CuOOH + H_2O + e^- \quad (1)$$

$$CuOOH + Glucose \longrightarrow Cu(OH)_2 + Gluconolactone \quad (2)$$

3.4 Effect of Scan Rate

Cyclic voltammograms of the 2D CuONSs@Pt foil electrode were performed at various scan rates ranging from 2 mVs^{-1} to 100 mVs^{-1} in 0.1 M NaOH solution **(Fig. 3C)**. The oxidation current gradually increases with increasing sweep rate as expected from the Randles-Sevcik equation. The oxidation current follows a good linear fit (R = 0.9986) with $I_{pc}(\mu A) = 1166.12 + 994.12 v\ (mVs^{-1})^{1/2}$ **(Fig. 3D)**. The linear relation between oxidation current and square root of scan rate indicates that the electro-oxidation reaction of glucose follows a diffusion-controlled process (1).

3.5 Optimization of Experimental Parameters

3.5.1 Effect of Cu^{2+} Ion Concentration

To optimize the performance of the glucose sensor, several different experimental parameters were varied. First, the effect of Cu^{2+} concentration, ranging from 2 mM to 30 mM, used to synthesize the CuO NSs was studied. The CVs of glucose oxidation with Pt electrodes modified with CuO synthesized at various Cu^{2+} concentrations are shown in **Fig. 4A**, and the figure inset illustrates the relationship between the peak oxidation current and the Cu^{2+} ion concentration. At a Cu^{2+} concentration of 10 mM, the CuO consists of well-developed 2D nanosheets, which enhance the rate of electron transfer, resulting in greater anodic current. When a higher concentration of Cu^{2+} is used to synthesize the CuO, agglomeration of CuO occurs during deposition. This agglomeration decreases the number of active sites, which decreases the reaction rate (**Fig. S1**). Therefore, a Cu^{2+} concentration of 10 mM was selected as an optimized concentration for further investigation in this manuscript.

3.5.2 Effect of Deposition Time

The deposition time also impacts the morphology of the CuO nanostructures. For this reason, CuO was deposited using the optimized 10 mM Cu^{2+} concentration at various times, and the current responses of the glucose oxidation reaction were measured **(Fig. 4B)**. Initially, the oxidation current of glucose was significantly improved when increasing the deposition time from 1 to 2 mins due to rapid electron transfer and catalytic activity of 2D CuO nanosheets. However, the anodic current decreases as the deposition time increase from 2 to 3 mins because longer deposition time increases agglomeration (**Fig. S2**), which inhibits the electron transfer rate and decreases the electrochemically active surface area of the catalyst. Thus, 2 mins was chosen as optimized time for deposition of the CuO nanosheets.

3.5.3 Effect of Deposition Potential

The influence of applied potential ranging 0.5 V to 2.5 V on the deposition during the synthesis of the CuO nanosheets was examined using the optimized 10 mM Cu^{2+} concentration for 2 mins of deposition time in acidic medium. The corresponding CVs of the modified electrodes are shown in **Fig. 4C**. The inset of **Fig. 4C** demonstrates the relationship between the oxidation current and deposition potential. The current signal of the glucose oxidation reaction rises appreciably as the deposition potential increases from 0.5 V to 1.5 V. At potentials more positive than 1.5 V, however, the current response gradually decreases. This trend is attributed to the formation of good morphology at 1.5 V, but at high potential there might be overlapping of CuO material (**Fig. S3**) and evolution of H_2 or O_2, which interferes in the deposition of CuO nanomaterials and decreases active binding sites and ultimately affects the reaction rate. Therefore, 1.5 V was selected as the optimal potential for the deposition of CuO nanosheets.

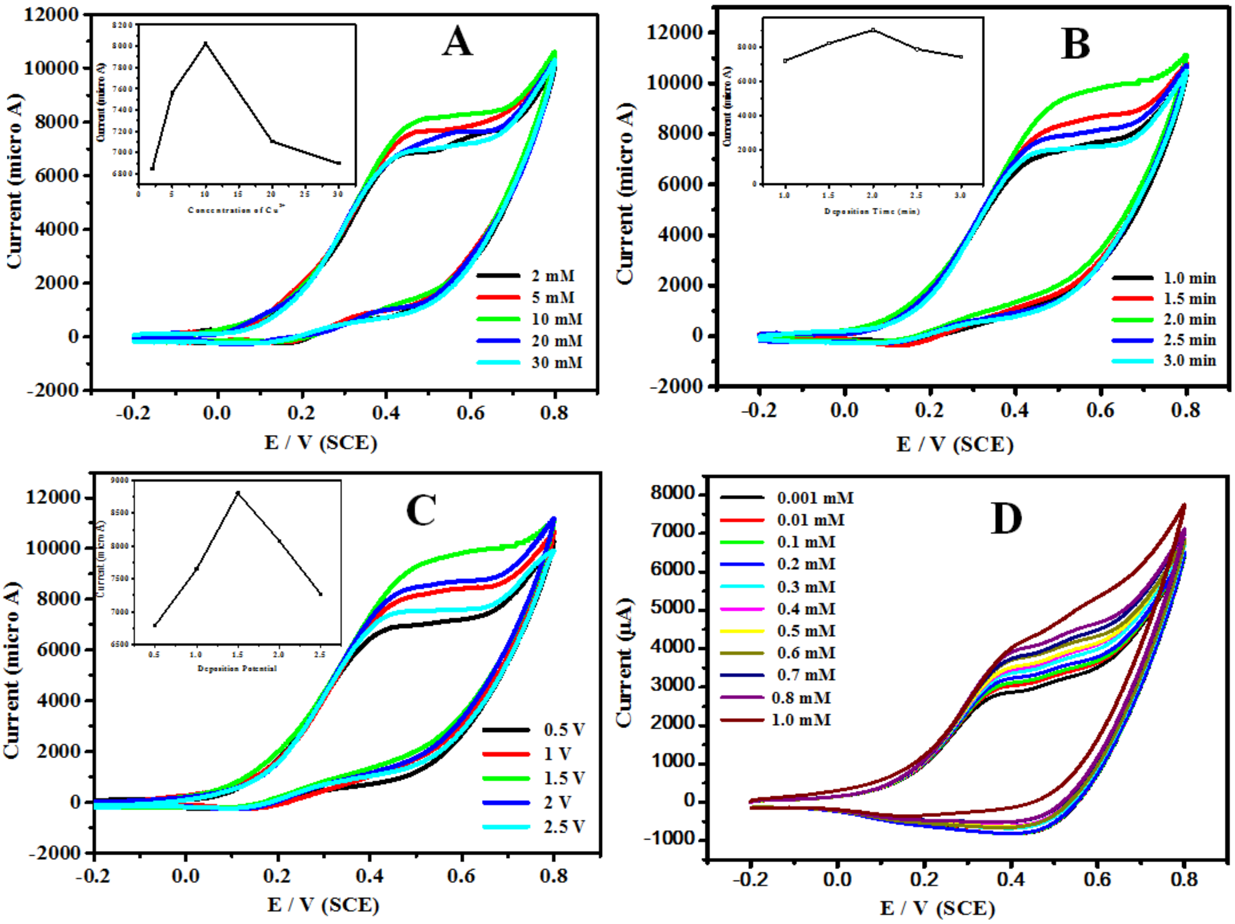

Figure 4. CVs of different Cu^{2+} ion concentrations **(A)**, deposition times **(B)**, deposition potentials **(C)**,and various concentrations **(D)** of glucose in 0.1 M NaOH solution at a scan rate of 50 mVs^{-1}.

3.6 Effect of Concentration and Calibration Curve

The effect of concentration on the glucose oxidation reaction was studied in 0.1 M NaOH solution. **Fig. 4D** displays voltammograms in electrolytes containing various glucose concentrations. The oxidation current linearly increases with increasing concentration of glucose. **Fig. 5A** shows the linear plot of the anodic current response versus concentrations of glucose. The 2D CuONSs@Pt exhibits good linearity from 0.001 mM to 1.0 mM and a high sensitivity of 2710 $\mu A.mM^{-1}.cm^{-2}$ which follows the equation I_{pa} (μA) = 3010.64 + 1292.11x (mM) (R = 0.998). The detection limit was found to be 0.8 μM.

The electrochemical performance of the sensors compared with previously reported non-enzymatic glucose sensors are shown in **Table 1**. The electrochemical sensor developed in this work possesses a very high sensitivity, broad linear range, and good limit of detection compared to other works. These excellent metrics are attributed to the large active surface area as well as the 2D morphology of the synthesized nanomaterial.

Table 1. The comparison of electrochemical activity with previously reported literature.

Electrode	Potential (V)	LOD (μM)	Linear range (mM)	Sensitivity ($\mu A.Mm^{-1}.cm^{-2}$)	Ref.
$CuS/Cu_2O/CuO/Cu$ foil	0.6	0.89	0.002-4.096	4262	37
Nano $CuBi_2O_4/CuO/FTO$	0.55	0.7	Up to 8	330	38
CuO/graphene/GCE	0.6	1	1 μM – 8 mM	1065	40
CuO NWs/Cu foam	0.35	0.3	0.001 – 18.8	2217.4	44
Cu_2O SCSM/PEDOT-MWCNTs	0.5	0.04	0.000495- 0.374	1439.1	50
CuO nanoplatelets@Cu foil	0.55	0.50	Up to 0.8	3490.7	51
CuTiPNPs-SPCE	0.6	7	25 μM - 2 mM	7.81	52
3D porous ZnO–CuO@FTO	0.7	0.21	Up to 1.6	3066.4	53
CuO-ZnONRs@FTO	0.62	0.40	Up to 8.45	2961.7	54
Au@Ni/C@GCE	0.1	15.7	0.5 - 10	23.17	55
Au/CuO@Cu foil	0.35	0.3	1.0 μM - 30 mM	708.7	56
2D CuO NSs@ Pt foil	0.42	0.8	0.001 - 1	2709.94	This work

3.7 Selectivity

Anti-interference properties of non-enzymatic glucose sensors are of great importance because other species such as ascorbic acid (AA), uric acid (UA), dopamine (DA), hydrogen peroxide (H_2O_2), and Na^+ are also present in blood serum and might interfere in the amperometric detection of glucose. Thus, the amperometric response of 0.5 mM glucose was measured with successive additions of the possibly interfering species AA, UA, DA, H_2O_2, and Na^+ at a concentration of 0.5 mM each in 0.1M NaOH. With all of these species, there is no significant change in the oxidation current of glucose (**Fig. 5B**). Consequently, the fabricated 2D CuONSs@Pt foil sensor exhibit excellent anti-interference ability due to the strong electrostatic repulsion force between negatively-charged CuO catalyst at the electrode surface and predominantly negatively-charged interfering species [35].

3.8 Reproducibility and Stability of the 2D CuONSs@Pt Sensor

In addition, the reproducibility and stability properties of glucose sensors are also essential for practical applications. The reproducibility of the 2D CuONSs@Pt foil sensor was determined by measuring the current response of the five modified electrodes through same procedure at room temperature for 2 mM glucose solution **(Fig 5C)**. The calculated value of relative standard deviation (RSD) for the oxidation current was 2.57%. To evaluate long-term stability of the sensor, the modified electrode was stored at room temperature for three weeks, and the current response measured was similar before and after storage. Specifically, the anodic current signal retained 96% of its original current **(Fig. 5D)**. The above results demonstrate that the modified 2D CuONSs@Pt foil sensor possesses excellent reproducibility and stability.

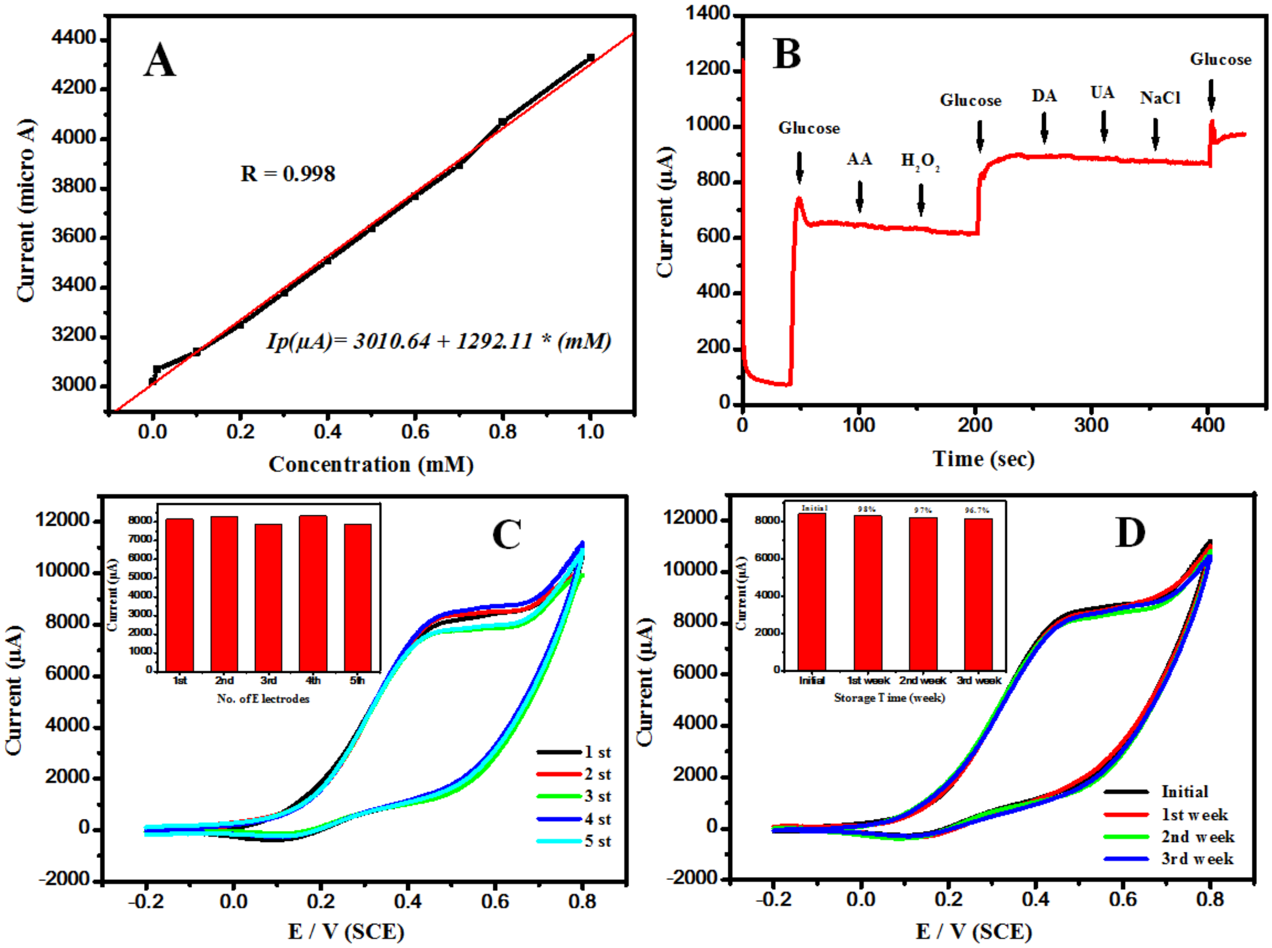

Figure 5. **(A)** Calibration plot of oxidation current (µA) and glucose concentrations (mM), **(B)** chronoamperometric (i-t) curve for various interfering species at 0.42 V, **(C)** CVs of Reproducibility and **(D)** stability in 2 mM glucose with 0.1 M NaOH solution at 50 mVs^{-1}.

4. Conclusions

In this manuscript, Pt electrodes modified with 2D CuO nanosheets were fabricated by a fast, simple, inexpensive, and stabilizer-free galvanostatic method that induced the direct electrooxidation of $Cu(NO_3)_2$ on Pt foil. Moreover, numerous parameters including Cu^{2+}ion concentration, deposition potential, deposition time, and pH of the precursor solution were investigated to understand how they affect the growth and morphology of the CuO nanosheets. The materials were characterized by FE-SEM, HR-TEM, XRD, and CV. The materials were then used to fabricate non-enzymatic glucose sensors that exhibit fast response times, high sensitivity, excellent selectivity, and good stability under a wide linear concentration range. These results are ascribed to the 2D nanostructure, which possess large electrochemical surface areas. Taken together, these findings demonstrate that 2D CuO nanosheets are a promising electrocatalytic material for the practical non-enzymatic detection of glucose.

Author's contribution

Jagdish C. Bhangoji: Conceptualization, Experimental Investigation, Writing-manuscript. **Dr. Suresh S. Shendage:** Supervision, Validation, Conceptualization, Methodology. **Christopher J. Barile:** Validation, Formal analysis, Manuscript review & editing

Declaration of Competing Interest

The authors declare that they have no any competing interests.

Acknowledgement

The authors thankful to research laboratory staff of the college for their kind support. Authors are also acknowledging to SAIF, IIT Bombay for SEM and TEM characterization techniques. Additionally, thanks to Department of Metallurgical engineering and Material science, IIT Bombay for XRD analysis technique. C. J. B. acknowledges that this material is based upon work supported by the National Science Foundation CAREER Award under Grant No. CHE2046105.

Reference

1. F. Zhou, Q. Wang, K. Huang, X. Jiang, Z. Zou, X. Xiong, Flame synthesis of NiO nanoparticles on carbon cloth: An efficient non-enzymatic sensor for glucose and formaldehyde, Microchemical Journal 159 (2020) 105505.
2. R. Madhuvilakku, R. Mariappan, S. Alagar, S. Piraman, Sensitive and Selective Non-enzymatic Detection of Glucose by Monodispersed NiO@S-doped Hollow Carbon Sphere Hybrid Nanostructures, Analytica Chimica Acta (2018), 10.1016/j.aca.2018.08.032.
3. D.U.J. Jung, R. Ahmad, Y. B. Hahn, Nonenzymatic flexible field-effect transistor-based glucose sensor fabricated using NiO quantum dots modified ZnO nanorods, J. Colloid and Interface Science 512 (2018) 21-28.
4. R. Ahmad, M. S. Ahn, Y. B. Hahn, Fabrication of a non-enzymatic glucose sensor field effect transistor based on vertically-oriented ZnO nanorods modified with Fe_2O_3, Electrochemistry Communications (2017), doi: 10.1016/j.elecom.2017.03.006.
5. Z. Lotfi, M. B. Gholivand, M. Shamsipur, Introduction of a non-enzymatic glucose sensor based on a g-C_3N_4/NiO/CuO nanocomposite, Analytical Biochemistry (2020), https://doi.org/10.1016/j.ab.2020.114062.
6. N. Amini, M. Shamsipur, A. Maleki, Construction of manganese oxide nanowire-like cluster arrays on a DNA template: application to detection of hydrogen peroxide, Bioelectrochemistry (2019), doi: https://doi.org/10.1016/j.bioelechem.2019.107419.
7. S. Daemi, S. Ghasemi, A. A. Ashkarran, Electrospun CuO-ZnO nanohybrid: Tuning the nanostructure for improved amperometric detection of hydrogen peroxide as a nonenzymatic sensor, J. Colloid and Interface Science 550 (2019) 180-189.
8. B. Xue, K. Li, S. Gu, L. Zhang, J. Lu, Ni foam-supported ZnO nanowires and Co_3O_4/$NiCo_2O_4$double-shelled nanocages for efficient hydrogen peroxide detection, Sensors and Actuators B 262 (2018) 828-836.

9. H. Zhang, S. Liu, Nanoparticles-assembled NiO nanosheets templated by graphene oxide film for highly sensitive non-enzymatic glucose sensing, Sensors and Actuators B: Chemical (2016), http://dx.doi.org/10.1016/j.snb.2016.07.126.
10. N. Pal, S. Banerjee, A. Bhaumik, A facile route for the syntheses of $Ni(OH)_2$ and NiO nanostructures as potential candidates for non-enzymatic glucose sensor, J. Colloid and Interface Science (2018), https://doi.org/10.1016/j.jcis.2018.01.027.
11. Z. Yu, H. Li, X. Zhang, N. Liu, X. Zhang, NiO/graphene nanocomposite for determination of H_2O_2 with a low detection limit, Talanta144 (2015) 1-5.
12. M.A.P. Papi, F. R. Caetano, M.F. Bergamini, L.H.M. Junior, Facile synthesis of a silver nanoparticles/polypyrrole nanocomposite for nonenzymatic glucose determination, Mater. Sci. Eng. C Mater BiolAppl 75 (2017) 88-94.
13. W. Meng, Y.Y. Wen, L. Dai, Z.X. He, L. Wang, A novel electrochemical sensor for glucose detection based on Ag@ZIF-67 nanocomposite, Sens. Actuators B Chem. 260 (2018) 852-860.
14. C. Li, Y. Su, X. Lv, H. Xia, H. Shi, X. Yang, J. Zhang, Y. Wang, Controllable anchoring of gold nanoparticles to polypyrrole nanofibers by hydrogen bonding and their application in nonenzymatic glucose sensors, Biosens. Bioelectron. 38 (2012) 402.
15. A. Liu, Q. Ren, T. Xu, M. Yuan, W. Tang, Morphology-controllable gold nanostructures on phosphorus doped diamond-like carbon surfaces and their electrocatalysis for glucose oxidation, Sensors and Actuators B: Chemical 162 (2012) 135–142.
16. Y. Fu, F. Liang, H. Tian, J. Hu, Nonenzymatic glucose sensor based on ITO electrode modified with gold nanoparticles by ion implantation, Electrochimica Acta 120 (2014) 314-318.
17. C. M. Zhang, Small naked Pt nanoparticles confined in mesoporous shell of hollow carbon spheres for high-performance nonenzymatic sensing of H_2O_2 and glucose. ACS Omega 3 (2018) 96-105.
18. L. Ma, Pt catalyzed formation of a Ni@Pt/reduced graphene oxide nanocomposite: preparation and electrochemical sensing application for glucose detection. Anal. Methods 10 (2018) 3845-3850.
19. D.Y. Zhai, Highly sensitive glucose sensor based on Pt nanoparticle/polyaniline hydrogel heterostructures. ACS Nano 7 (2013) 3540-3546.
20. K. Dhara, J. Stanley, R. T, B.G. Nair, S.B.T.G, Pt-CuO nanoparticles decorated reduced graphene oxide for the fabrication of highly sensitive non-enzymatic disposable glucose sensor, Sens. Actuators B: Chem 195 (2014) 197.
21. M.F. Hossain, J. Y. Park, Plain to point network reduced graphene oxide-activated carbon composites decorated with platinum nanoparticles for urine glucose detection, Scientific Reports 6 (2016) 21009.
22. H. Bai, M. Han, Y. Du, J. Bao, Z. Dai, Facile synthesis of porous tubular palladium nanostructures and their application in a nonenzymatic glucose sensor, Chem. Commun. 46 (2010) 1739–1741.
23. H. Y. Huang, P. Y. Chen, PdNi- and Pd-coated electrodes prepared by electrodeposition from ionic liquid for nonenzymatic electrochemical determination of ethanol and glucose in alkaline media, Talanta 83 (2010) 379.

24. X. Chen, G. Wu, J. Chen, X. Chen, Z. Xie, X. Wang, Synthesis of Clean and Well-Dispersive Pd Nanoparticles with Excellent Electrocatalytic Property on Graphene Oxide, J. American Chemical Society 133 (2011) 3693-3695.
25. B. Singh, F. Laffir, T. Mccormac, E. Dempsey, PtAu/C based bimetallic nanocomposites for non-enzymatic electrochemical glucose detection, Sens. Actuators B Chem. 150 (2010) 80-92.
26. C.C. Shen, J. Su, X.Z. Li, J.J. Luo, M.H. Yang, Electrochemical sensing platform based on Pd-Au bimetallic cluster for non-enzymatic detection of glucose, Sens. Actuators B Chem. 209 (2015) 695-700.
27. K.K. Naik, A. Gangan, B. Chakraborty, C.S. Rout, Superior non-enzymatic glucose sensing properties of Ag/Au-$NiCo_2O_4$ nanosheets with insight from electronic structure simulations, Analyst 143 (2018) 571-579.
28. R. Yuan, H. Li, X. Yin, L. Zhang, J. Lu Stable controlled growth of 3D CuO/Cu nanoflowers by surfactant-free method for non-enzymatic hydrogen peroxide detection, J. Materials Science & Technology (2017), https://doi.org/10.1016/j.jmst.2017.11.030.
29. Y. Liu, W. Zhao, X. Li, J. Liu, Y. Han, J. Wu, X. Zhang, Y. Xu, Hierarchical α-Fe_2O_3 microcubes supported on Ni foam as non-enzymatic glucose sensor, Applied Surface Science 512 (2020) 145710.
30. S.F. Chong, K.A. Razak, N.M. Nor, N.S. Ridhuan, N.D. Zakaria, Electrochemical Glucose Detection using Screen-Printed Carbon Electrode Modified Silica-Encapsulated Iron Oxide Nanoparticles, Materials Today: Proceedings 17 (2019) 1189–1196.
31. J. Cai, S. Ding, G. Chen, Y. Sun, Q. Xie, In situ electrodeposition of mesoporous aligned α-Fe_2O_3 nanoflakes for highly sensitive nonenzymatic H_2O_2 sensor, Applied Surface Science (2018), doi: https://doi.org/10.1016/j.apsusc.2018.06.108.
32. L. Hao, S.S. Li, J. Wang, Y. Tan, L. Bai, A. Liu, MnO_2/multi-walled carbon nanotubes-based nanocomposite with enhanced electrocatalytic activity for sensitive amperometric glucose biosensing, J. Electroanalytical Chemistry 878 (2020) 114602.
33. K. Sankarasubramanian, K. Justice Babu, P. Soundarrajana, T. Logu, G. Gnanakumar, K. Ramamurthi, K. Sethuraman, S.M. Senthil, Kumar A new catalyst Ti doped CdO thin film for non-enzymatic hydrogen peroxide sensor application, Sensors & Actuators: B. Chemical 285 (2019) 164–172.
34. R. Ramachandran, C. Zhao, M. Rajkumar, K. Rajavel, P. Zhu, W. Xuan, Z.X. Xu, F. Wang, Porous nickel oxide microsphere and $Ti_3C_2T_x$ hybrid derived from metal-organic framework for battery-type supercapacitor electrode and non-enzymatic H_2O_2 sensor, Electrochimica Acta 322 (2019) 134771.
35. R.K. Das, A.K. Golder, Use of plant-based analytes for the synthesis of NiO nanoparticles in catalyzing electrochemical H_2O_2 production, J. Electroanalytical Chemistry (2018), doi:10.1016/j.jelechem.2018.05.029.
36. W. Liu, W. Zhan, X. Jia, Q. Liu, R. Chen, D. Li, Y. Huang, G. Zhang, H. Ni, Rapid synthesis of vertically-aligned zinc oxide nanorods on stainless steel for non-enzymatic glucose and H_2O_2 photoelectrochemical sensor, Applied Surface Science 480 (2019) 341–348.

37. C. Wei, X. Zou, Q. Liu, S. Li, C. Kang, W. Xiang, A highly sensitive non-enzymatic glucose sensor based on CuS nanosheets modified Cu_2O/CuO nanowire arrays, Electrochimica Acta 334 (2020) 135630.
38. C.H. Wu, E. Onno, C.Y. Lin, CuO nanoparticles decorated nano-dendrite-structured $CuBi_2O_4$ for highly sensitive and selective electrochemical detection of glucose, Electrochimica Acta 229 (2017) 129–140.
39. J. Bai, X. Bo, C. Luhana, L. Guo, A novel material based on cupric(II) oxide/macroporous carbon and its enhanced electrochemical property, Electrochimica Acta 56 (2011) 7377– 7384.
40. Y.W. Hsu, T.K. Hsu, C.L. Sun, Y.T. Nien, N.W. Pu, M.D. Ger, Synthesis of CuO/graphene nanocomposites for nonenzymatic electrochemical glucose biosensor applications, Electrochimica Acta 82 (2012) 152– 157.
41. R. Eliot, CuO nanospheres based nonenzymatic glucose sensor, Electroanalysis 20 (2008) 2482–2486.
42. X. Gou, A very facile strategy for the synthesis of ultrathin CuO nanorods towards non-enzymatic glucose sensing. New Journal of Chemistry 42 (2018) 6364–6369.
43. D. Chirizzi, M.R. Guascito, E. Filippo, C. Malitesta, A. Tepore, A novel nonenzymatic amperometric hydrogen peroxide sensor based on CuO@Cu_2O nanowires embedded into poly (vinyl alcohol), Talanta 147 (2016) 124-131.
44. Z. Li, Y. Chen, Y. Xin, Z. Zhang, Sensitive electrochemical nonenzymatic glucose sensing based on anodized CuO nanowires on three-dimensional porous copper foam, Scientific Reports 5 (2015) 16115.
45. M. Liu, R. Liu, W. Chen, Graphene wrapped Cu_2O nanocubes: non-enzymatic electrochemical sensors for the detection of glucose and hydrogen peroxide with enhanced stability, Biosens. Bioelectron. 45 (2013) 206-212.
46. Z. H. Ibupoto, K. Khun, V. Beni, X. Liu, M. Willander, Synthesis of novel CuO nanosheets and their non-enzymatic glucose sensing applications. Sensors 13 (2013) 7926–7938.
47. L.L. Tian, Fabrication of CuO nanosheets modified Cu electrode and its excellent electrocatalytic performance towards glucose. Appl. Surf. Sci. 283 (2013) 947–953.
48. W. Wang, L. Zhang, S. Tong, X. Li, W. Song, Three-dimensional network films of electrospun copper oxide nanofibers for glucose determination. Biosens. Bioelectron. 25 (2009)708–714.
49. Xiaolin Wang, Enli Liu, Xiaoli, Zhang Non-enzymatic glucose biosensor based on copper oxide-reducedgraphene oxide nanocomposites synthesized from water-isopropanol solution, Electrochimica Acta 130 (2014) 253–260.
50. Li Na Wu, Jing Ping Zhong, Muhammad Waqas, Zhe Jiang, You-Jun Fan, Yue Sun, Jia Li, Wei Chen, Controllable synthesis of six corner star-like Cu_2O/PEDOT-MWCNT composites and their performance toward electrochemical glucose sensing, Electrochimica Acta 318 (2019) 837-846.
51. Juan Wang, Wei De Zhang, Fabrication of CuO nanoplatelets for highly sensitive enzyme-free determination of glucose, Electrochimica Acta 56 (2011) 7510–7516.

52. Daniel Martín-Yerga, Javier Carrasco-Rodríguez, José Luis G. Fierro, Francisco Javier García Alonso, Agustín Costa-García, Copper-modified titanium phosphate nanoparticles as electrocatalyst for glucose detection, Electrochimica Acta 229 (2017) 102–111.
53. Chunyang Zhou, Lin Xu, Jian Song, Ruiqing Xing, Sai Xu, Dali Liu, Hongwei Song, Ultrasensitive non-enzymatic glucose sensor based on three-dimensional network of ZnO-CuO hierarchical nanocomposites by electrospinning, Scientific Reports 4, (2014) 7382.
54. Rafiq Ahmad, Nirmalya Tripathy, Min Sang Ahn, Kiesar Sideeq Bhat, Tahmineh Mahmoudi, Yousheng Wang, Jin Young Yoo, Dae Wook Kwon, Hwa Young Yang, Yoon Bong Hahn, Highly Efficient Non-Enzymatic Glucose Sensor Based on CuO Modified Vertically-Grown ZnO Nanorods on Electrode, Scientific Reports 7 (2017) 5715.
55. Xuejin Gao, Xinzhao Du, Danpye Liu, Huihui Gao, Pu Wang, Jun Yang, Core-shell gold-nickel nanostructures as highly selective and stable nonenzymatic glucose sensor for fermentation process, Scientific Reports 10 (2020) 1365.
56. Zhenzhen Li, Yanmei Xin, Zhonghai Zhang, Hongjun Wu, Peng Wang, Rational design of binder-free noble metal/metal oxide arrays with nanocauliflower structure for wide linear range nonenzymatic glucose detection, Scientific Reports 5 (2015) 10617.